Evaluation of Fog Effects on Optical Camera Communications Link

Vicente Matus*, Shivani Rajendra Teli†, Victor Guerra*,
Cristo Jurado-Verdu*, Stanislav Zvanovec†, Rafael Perez-Jimenez*
*IDeTIC-ULPGC, Las Palmas de Gran Canaria, Spain
†Czech Technical University in Prague, Czech Republic
vmatus@idetic.eu, telishiv@fel.cvut.cz, vguerra@idetic.eu,
cjurado@idetic.eu, xzvanove@fel.cvut.cz, rperez@idetic.eu

***Abstract*—The applications of Optical Camera Communications (OCC) have been tested for vehicular communications, Internet-of-things, and other outdoor scenarios due to the vast availability of standard camera equipment. The outdoor channel is, however, affected by atmospheric conditions, ranging from the presence of particles or water drops in the air to thermally induced fluctuations of the refractive index (turbulence). In this work, we experimentally investigate the influence of fog on an OCC link exploiting rolling shutter cameras and using red-green-blue channels inside a laboratory chamber featuring a fog machine. The analysis is performed using the Pearson's correlation coefficient between test and reference signals as a measure of similarity or decay of the signal attenuation of fog associated with atmospheric visibility.**

***Index Terms*—Optical camera communications (OCC), fog, meteorological visibility, experimental outdoor OCC.**

I. Introduction

Optical Camera Communications (OCC) using Complementary Metal-Oxide-Semiconductor (CMOS) camera as receiver (Rx) has been investigated as one of the Visible Light Communication (VLC) schemes [1]. OCC implemented within internet of things (IoT) environments provides multiple functionalities of vision, data communications, localization and motion detection [2]–[4] used in various IoT-based network applications including device-to-device communications [5], mobile atto-cells [6], vehicle-to-everything (V2X) [7], smart environments (cities, industries, offices, homes, surveillance), etc. [8]. A popular way to implement OCC in the Rx is by using the rolling shutter (RS) acquisition mechanism of CMOS, in which the sensor captures the image row-by-row with a delay between each line [9]. The camera captures a set of states of the signal from the VLC Light Emitting Diode (LED) transmitter (Tx) based on the timings of the RS scanning. These are governed by the CMOS chip's fixed row-shift time (t_{rs}) and the software-defined exposure time (t_{exp}) [10], as shown in Fig. 1.

The widespread use of LED as taillights, brake lights, headlights, traffic signals, lighting infrastructures, display communications, and cameras for safety and comfort applications has reached into fields such as sensor networks, automotive and industrial facilities. In outdoor VLC environments, the intensity-based detection method [8], [11] fails to produce reliable data detection due to the presence of high-power external light sources such as sunlight. The communications performance is also strongly dependent on weather conditions over the optical channel, such as rain, snow, and fog, because these conditions cause a severe loss on the LED transmission quality. In particular, foggy weather causes either poor or no communication, thus making LED-photodetector (PD) based VLC impractical. A comprehensive study of VLC and OCC outdoor links in terms of atmospheric attenuation under fog conditions needs to be conducted. To this end, [12] investigated the success rate of received bits of an OCC link for vehicular communications between red brake light and camera varying the modulation index of On-off keying (OOK) setting. They experimentally tested the setup in a laboratory chamber. [13] studied the influence of rain and fog on VLC based V2V. They derived a path-loss model based on Mie's theory aided by Zemax software to create simulations. They obtained expressions for the maximum achievable distances for a desired value bit-error-ratio (BER). Authors in [14] experimentally investigated the effect of light and heavy fog employing a single red LED as Tx and three PD units and a Fresnel lens as the Rx. With this setup, they overcome the attenuation due to the gain the lens gives. In [15], the characterization of maritime fog and the effects on VLC is studied also using Mie's theory to model both scattering and phase functions since the size of water particles is proportional to the wavelengths of visible light. They obtained the attenuation over the spectrum of white LED employed for different distances.

OCC deployment in particular applications such as vehicle-to-vehicle (V2V), vehicle-to-infrastructure (V2I or I2V) and vehicle-to-everything (V2X or X2V) is of increased interest [16], [17], due possibly to the use of pre-existing camera-based infrastructures, such as traffic camera networks, security cameras, or the already installed car dashboard cameras. Authors in [16], [17] investigated the use of high-speed CMOS image sensors for automotive applications, with the primary aim of increasing the data throughput up to 10 Mbps. However, the concept was based on a custom-made combination of image pixels and communication pixels, not based on off-the-shelf

This paper has been supported by the European Union's Horizon 2020 research and innovation program under the Marie Skłodowska-Curie grant agreement No 764461 (VisIoN Project)

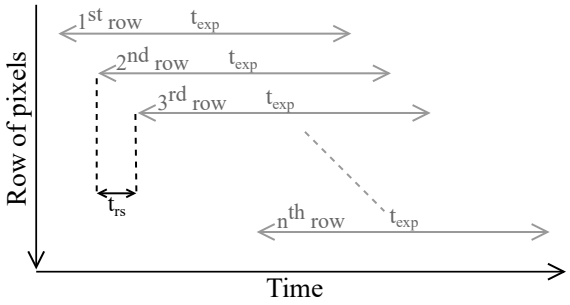

Fig. 1. Important parameters of line scan timing in rolling shutter CMOS camera.

CMOS cameras.

The recent OCC research is mainly focused on data rate enhancement and establishing reliable link qualities. However, OCC links, when deployed for outdoor applications, mainly need to focus on the effect of atmospheric conditions on the link performance, which is sparsely reported in the literature [18]. Works addressing channel characterization in outdoor OCC links are sparse compared to the vast research of this topic within Free Space Optics (FSO), which use collimated beams on particular wavelengths (850 nm or 1550 nm) instead of diffuse wideband light in the visible spectrum.

This paper aims to explore the capabilities of OCC in the presence of fog. The experiments carried out for this work were done using an atmospheric chamber, equipped with a laser source and power meter to estimate the fog level across the chamber by means of meteorological visibility (V_M). A self-made red-green-blue (RGB) LED lamp with a VLC front-end, and a low-cost CMOS camera with RS acquisition comprise the system.

The content of this paper is structured as follows. Section II presents the experimental setup and describes the methodology used. Section III shows the results obtained from data processing and related discussion. Finally, conclusions are drawn in Section IV.

II. Experimental Setup and Methods

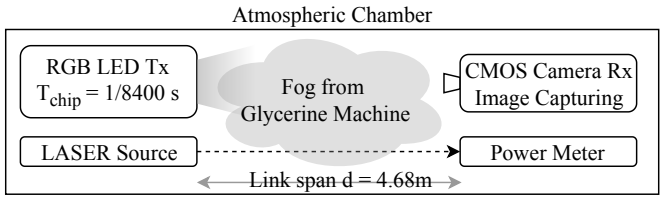

Fig. 2. Diagram of the experimental setup.

The effects of fog over an RS-based OCC unidirectional link were studied using a laboratory chamber at the facilities of the Czech Technical University in Prague. Since RS takes advantage of the line scanning, the impact of this atmospheric condition can be positive if the projection of the Tx area over the camera sensor increases its dimensions due to scattering. On the other hand, the attenuation associated with the presence of particles in the air has a negative impact that must be studied.

A light source's radiation pattern can be modeled as a Lambertian function of order m [8], with a transmitted power $P_{Tx}(t)$. Then the received power $P_{Rx}(t)$ can be expressed as:

$$P_{Rx}(t) = P_{Tx}(t) \cdot \frac{m+1}{2\pi} \cdot \cos\theta \frac{A_{lens} \cos\Psi}{d^2}, \qquad (1)$$

where d is the Tx-Rx distance, θ the emission angle, Ψ the incident angle, and A_{lens} is the area of the main lens of the camera. The RS mechanism makes the energy integrated by the i^{th} row E_i to be as:

$$E_i = \int_{i \cdot t_{rs}}^{i \cdot t_{rs} + t_{exp}} \frac{P_{Rx}(t)}{\sum_j^v \sum_k^h M_{j,k}} dt, \qquad (2)$$

where h (columns) and v (rows), are the dimensions of the CMOS sensor, and $M_{[v \times h]}$ is the mask of pixels where the shape of the transmitting surface is projected.

The emulation of fog in this work was done using a Glycerine machine. For evaluating the channel attenuation, the related meteorological visibility (V_M), was derived from the measurement of laser power intensity of a $625nm$ and $2mW$ beam across the span of the chamber.

The VLC Tx lamp is set to transmit a beacon signal formed by pulses of each of the RGB colors, followed by a black (off state) pulse. The pure color pulses allows estimating the mismatch between the spectra of the LED and the Bayer filter of the camera, which causes an inter-channel cross-talk [19]. The Rx camera was programmed to make image captures at $t_{exp} = 60\mu s$. After taking reference measurements with clear conditions, we manipulated the atmospheric conditions while sustaining the beacon transmission and capture processes. The key experiment parameters are listed in Table I and the diagram of experimental setup is shown in Fig. 2.

TABLE I
System parameters.

Description	Values
Capture device	Raspberry Pi + Picamera V2 module
camera resolution	3280×2464 px
shutter speed	$60\mu s$
Tx	RGB LED strips ($5 \times 5mm$ SMD chips)
Tx symbol rate	$1/8400Hz$
OCC link span	$4.68m$

Transmitters used were made out of arrays of RGB LED connected to a microcontroller model ATMega328p, and a switching circuit based on transistors. We installed the LED strips on aluminum rails with white meth-acrylate diffuser. The circuitry makes the RGB channels to repeatedly emit the beacon signal at a rate that is set by software in the microcontroller.

The receivers were made using the development board Raspberry Pi with PiCamera V2. The CMOS sensor (Sony IMX219PQH5-C [20]) fixed internal structure is set to have a row-shift time $t_{rs} = 18.904\mu s$. The exposure time was set to $t_{exp} = 60\mu s$.

For the later analysis of data, the reference images and the captures taken in fog conditions, denoted as reference and test image sequences respectively, are taken through processes including the detection of region of interest (ROI) in the image, the estimation of inter-channel cross-talk, and the calculation of the Pearson's correlation coefficient (ρ_{XY}) between test and reference image sequences as a measure of similarity between both.

The detection of ROI in OCC consists of determining the relevant group of pixels from which the Rx can decode information. The amount of rows forming this group is proportional to the number of different states of the lamp that can be decoded. Also, if multiple columns of pixels form the region of interest, the information inside the rows can be averaged, allowing to filter noise.

In this work, the ROI is first manually extracted from the reference group and, since the alignment is maintained, the test group's regions of interest are extracted re-using the coordinates. For estimating the impact of fog on the dimensions of the ROI, a detection algorithm is performed, and ROI limits are determined by finding the pixels with an intensity of 20% of the extinction ratio. We chose this limit after computing the algorithm for a range of values and selected the result with the minimum amount of results with dimensions smaller than the reference ROI, considered to be spurious.

Afterward, from the extraction of ROI, $Signal_{[Nx3]}$ is obtained, where N is the number of rows of the ROI, and 3 is related to the RGB channels. From the reference ROI, a template of one beacon signal of the transmitter is saved as $Ref_{[Mx3]}$, where M is the number of rows used by the beacon.

The cross-talk between RGB channels is then estimated by manually analyzing the reference pixels containing information from pure R, G, and B pulses of the LED. Then, the matrix $H^{-1}_{[3\times3]}$ is used to clean all the data, giving the cleaned signals $Ref'_{[Mx3]}$ and $Signal'_{[Nx3]}$. These are later evaluated by Pearson's correlation coefficient.

III. Results

One important impact of fog over OCC can be the expansion of ROI due to the scattering of light resulting in an apparent enlarged image of the transmitter. For this reason, the influence of fog on the dimensions of detected ROI were studied. In this case, the algorithm described in Section II was used to detect the width of ROI, as shown in Fig. 3. The algorithm was not used for the estimation of height or ROI since the black pulses of the beacon can be considered as pixels without information. Nevertheless, the expansion in one axis should be equal to the other one.

The ROI widths of the image sequences in different fog levels were estimated, and the difference of pixel columns with respect to reference ROI was obtained and is shown for different scales of V_M in Fig. 4. In this image, we can see that there is an expansion of the ROI at low visibility values, although minimal if it is compared to the dimensions of the ROI (229 by 25 pixels).

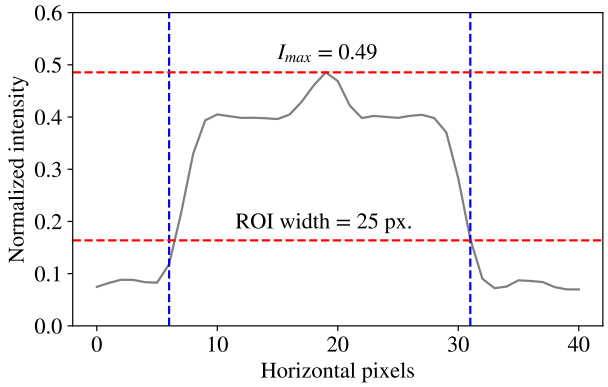

Fig. 3. Output from the estimation of ROI dimensions of an example test signal. Red lines are: (upper) peak intensity, and (lower) the decay of 20% of the extinction ratio. Blue lines are the intersection of red lines and the grayscale intensity profile of lamp (horizontal axis).

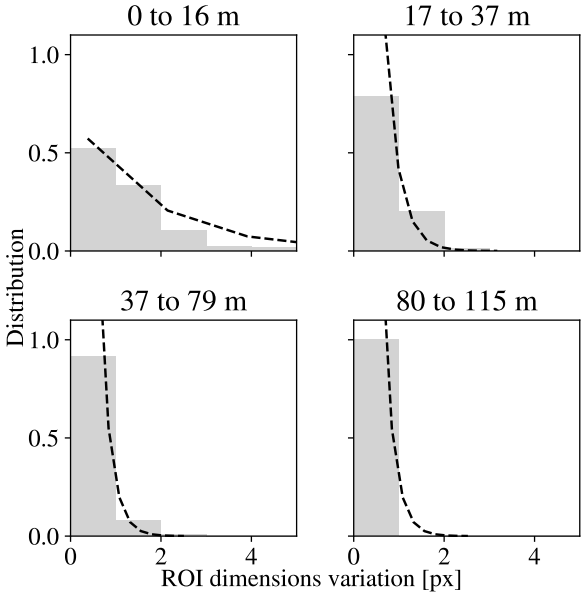

Fig. 4. Histograms and estimated distribution of the detected ROI dimensions variation with respect to reference, separated by equally sized groups according to the level of meteorological visibility V_M at the capture.

The analysis of Pearson's correlation coefficient between cleaned test data ($Signal'_{[N\times3]}$) and cleaned reference data ($Ref'_{[N\times3]}$) was done all along the extracted ROI, giving a periodic curve in which the peaks correspond to the positions of the reference signal that match the phase of the test signal, as shown in Fig. 5. The highest value of ρ_{XY} is saved as the similarity of the picture compared to the reference image.

By saving the peak values of $\rho_{X,Y}$ of each image, and meteorological visibility at capture, the relation of these two variables can be studied, as shown in Fig. 6. The scatter plot

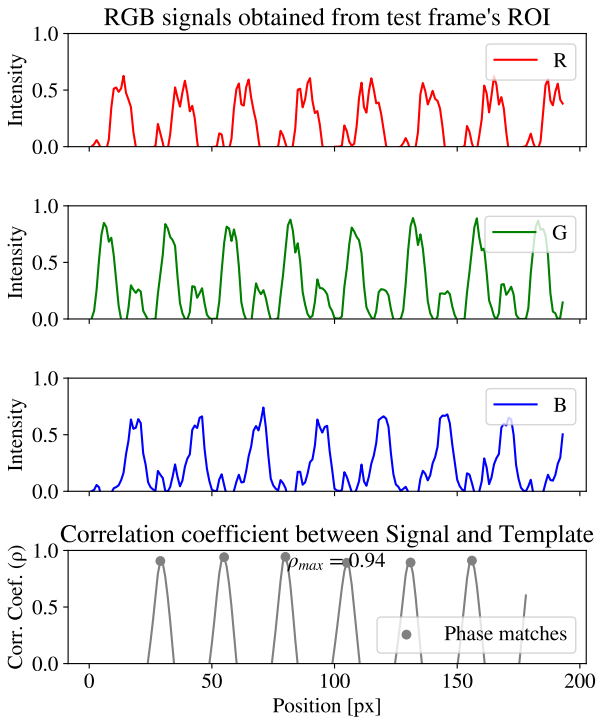

Fig. 5. Example of $Signal'_{[N\times3]}$ obtained from test frame and its correlation coefficient with $Ref'_{[N\times3]}$ along the height of ROI.

obtained shows an obvious trend of the correlation coefficient to decrease when V_M is low because the fog attenuates the signal and then the SNR must decrease, and then the similarity to the reference signal is lowered. The figure manifests that above the level of $V_M \approx 40m$ the test signal remains similar to the reference. Then, below this level, the similarity is damaged. From the non-parametrical regression LOESS of parameter $\alpha = 0.5$ [21], can be seen that the correlation coefficient drops fast bellow the level of $V_M \approx 20m$.

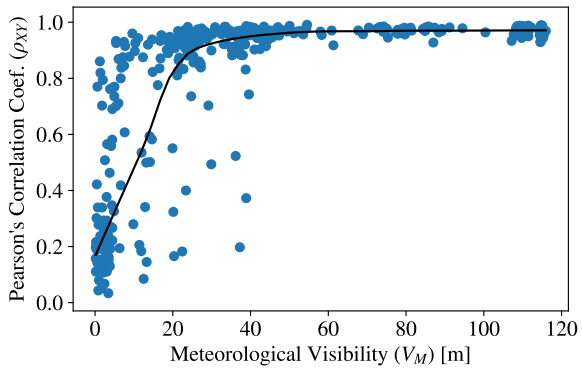

Fig. 6. Peak values of $\rho_{X,Y}$ obtained from the test group with respect to $Ref'_{[N\times3]}$, plotted against V_M. LOESS regression is shown for parameter $\alpha = 0.5$ [21].

IV. Conclusions

This paper presents a study on the influence of the presence of fog over an experimental setup of an OCC unidirectional link in a 5-m-long laboratory chamber. From our results, it was shown that the presence of fog impaired the received signal's Pearson's correlation coefficient with respect to reference signals when the meteorological visibility falls below 40 m, and $\rho_{X,Y}$ decreases severely when V_M is under 20 m. It was also presented that the ROI detection process delivered dimensions of the region of interest that were similar to the reference when the meteorological visibility decreased, although for values of V_M lower than 10 m the algorithm failed to detect the ROI dimensions consistently. With these results, we can assume that the presence of fog causes an attenuation that must be compensated for V_M values underneath 40 m, and that also the presence of fog does not make OCC able to use larger groups of pixels for signal detection.

Acknowledgment

V. M. thanks the help received from Jan Bohata, Petr Chvojka, and Dmytro Suslov at the Czech Technical University in Prague, and Elizabeth Eso from Northumbria University in Newcastle Upon Tyne.

References

[1] W. A. Cahyadi, Y. H. Kim, Y. H. Chung, and C. Ahn, "Mobile phone camera-based indoor visible light communications with rotation compensation," *IEEE Photonics Journal*, no. 2, April 2016.

[2] M. J. Jang, "IEEE 802.15 WPAN 15.7 amendment - optical camera communications study group (SG 7a)," *IEEE 802.15 WPAN*, 2019 [Online accessed 5 October 2019].

[3] S. R. Teli, S. Zvanovec, and Z. Ghassemlooy, "Performance evaluation of neural network assisted motion detection schemes implemented within indoor optical camera based communications," *Opt. Express*, no. 17, Aug 2019.

[4] P. Chavez-Burbano, S. Vitek, S. R. Teli, V. Guerra, J. Rabadan, R. Perez-Jimenez, and S. Zvanovec, "Optical camera communication system for internet of things based on organic light emitting diodes," *Electronics Letters*, no. 6, 2019.

[5] S. V. Tiwari, A. Sewaiwar, and Y. H. Chung, "Optical bidirectional beacon based visible light communications," *Opt. Express*, no. 20, Oct 2015.

[6] S. Pergoloni, M. Biagi, S. Colonnese, R. Cusani, and G. Scarano, "Coverage optimization of 5G atto-cells for visible light communications access," in *2015 IEEE International Workshop on Measurements Networking (M N)*, Oct 2015.

[7] M. Boban, A. Kousaridas, K. Manolakis, J. Eichinger, and W. Xu, "Connected roads of the future: Use cases, requirements, and design considerations for vehicle-to-everything communications," *IEEE Vehicular Technology Magazine*, no. 3, Sep. 2018.

[8] Z. Ghassemlooy, L. N. Alves, S. Zvanovec, and M.-A. Khalighi, *Visible light communications: theory and applications*. CRC press, 2017.

[9] T. Nguyen, Chang Hyun Hong, Nam Tuan Le, and Y. M. Jang, "High-speed asynchronous optical camera communication using led and rolling shutter camera," in *2015 Seventh International Conference on Ubiquitous and Future Networks*, July 2015.

[10] T. Kuroda, *Essential Principles of Image Sensors*. CRC Press, 2017.

[11] Y. H. Kim and Y. H. Chung, "Experimental outdoor visible light data communication system using differential decision threshold with optical and color filters," *Optical Engineering*, no. 4, 2015.

[12] E. F. Eso, A. Burton, N. B. Hassan, M. M. Abadi, Z. Ghassemlooy, and S. Zvanovec, "Experimental investigation of the effects of fog on optical camera-based vlc for a vehicular environment," in *2019 15th International Conference on Telecommunications (ConTEL)*, July 2019.

[13] M. Elamassie, M. Karbalayghareh, F. Miramirkhani, R. C. Kizilirmak, and M. Uysal, "Effect of fog and rain on the performance of vehicular visible light communications," in *2018 IEEE 87th Vehicular Technology Conference (VTC Spring)*, June 2018.

[14] Y. H. Kim, W. A. Cahyadi, and Y. H. Chung, "Experimental demonstration of VLC-based vehicle-to-vehicle communications under fog conditions," *IEEE Photonics Journal*, no. 6, Dec 2015.

[15] X. Tian, Z. Miao, X. Han, and F. Lu, "Sea fog attenuation analysis of white-led light sources for maritime VLC," in *2019 IEEE International Conference on Computational Electromagnetics (ICCEM)*, March 2019.

[16] T. Yamazato, I. Takai, H. Okada, T. Fujii, T. Yendo, S. Arai, M. Andoh, T. Harada, K. Yasutomi, K. Kagawa, and S. Kawahito, "Image-sensor-based visible light communication for automotive applications," *IEEE Communications Magazine*, no. 7, July 2014.

[17] I. Takai, S. Ito, K. Yasutomi, K. Kagawa, M. Andoh, and S. Kawahito, "LED and CMOS image sensor based optical wireless communication system for automotive applications," *IEEE Photonics Journal*, no. 5, Oct 2013.

[18] A. Islam, M. T. Hossan, and Y. M. Jang, "Convolutional neural network scheme-based optical camera communication system for intelligent internet of vehicles," *International Journal of Distributed Sensor Networks*, no. 4, 2018.

[19] C. Jurado-Verdu, V. Matus, J. Rabadan, V. Guerra, and R. Perez-Jimenez, "Correlation-based receiver for optical camera communications," *Opt. Express*, no. 14, Jul 2019.

[20] Sony Corporation, *IMX219PQH5-C, Diagonal 4.60 mm (Type 1/4.0) 8 Mega-Pixel CMOS Image Sensor with Square Pixel for Color Cameras, Datasheet*. Sony Corporation, 2014.

[21] W. S. Cleveland and S. J. Devlin, "Locally weighted regression: An approach to regression analysis by local fitting," *Journal of the American Statistical Association*, no. 403, 1988.